

UV-Bright Nearby Early Type Galaxies Observed in the Mid-Infrared: Evidence for a Multi-Stage formation History by Way of *WISE* and *GALEX* Imaging

SARA M. PETTY,^{1,2} JAMES D. NEILL,³ TOM JARRETT,⁴ ANDREW BLAIN,⁵ DUNCAN FARRAH,¹ R.M. RICH,² CHAO-WEI TSAI,⁴ DOMINIC BENFORD,⁶ CARRIE BRIDGE,³ SEAN LAKE,² FRANK MASCI,⁷ AND EDWARD WRIGHT²

¹Virginia Tech, USA

²University of California, Los Angeles, USA

³Caltech, USA

⁴University of Cape Town, South Africa

⁵University of Leicester, UK

⁶NASA, Goddard Space Flight Center, USA

⁷IPAC, Caltech, USA

ABSTRACT

At $z \lesssim 0.1$, 10% of massive elliptical galaxies exhibit a substantial excess of ultraviolet emission over what is expected from their old stellar populations (the ‘UVX’). We explore the source and radial distribution of UVX in 49 nearby E/S0-type galaxies by measuring their extended photometry in the UV to mid-IR with *GALEX*, SDSS and *WISE*. We find a 1 magnitude separation of color between the inner and outer regions. Via careful modelling, we show that this color difference is most readily explained by a ~ 0.5 to 2 Gyr age difference. This is consistent with ‘inside-out’ formation: rapid star formation in the core at > 4 Gyr ago, and at least one later stage starburst event coinciding with $z \sim 1$.

1. BACKGROUND AND SAMPLE

That some early type galaxies (ETGs) are strong emitters of UV is a decades-old mystery. In ETGs, the UVX appears as a sudden increase in the flux in spectral energy distributions (SEDs) blueward of 2500 Å. Possible sources of UVX include recent star formation, metal-poor > 10 Gyr-old horizontal branch (HB) stars, younger metal-rich HB stars, or a combination of these (see O’Connell 1999, for a review). By understanding how ETGs evolved to their present state, we can determine the major sources of mass-building over cosmological history. The theories need to integrate many factors, including the morphologies and age-metallicity differences observed between more and less massive ETGs. Mergers play an important role in explaining these factors. For example, dissipational (gas-rich) mergers would seed new star formation, while a dissipationless (gas-poor) merger would add mass through minor merging with quiescent systems. Merging is suspected to play a roll in an inside-out cessation, a core forms through very rapid starbursts at high redshifts, fueled by wet-merging. At later epochs, major multi-stage growth form the outer regions via minor mergers and accretion of hot gas from the immediate environment (e.g., Daddi et al. 2005; Nelson et al. 2012).

We use imaging from the recently completed *Wide-field Infrared Survey Explorer* (*WISE*) mid-IR imaging to explore the UV to mid-IR color-space of ETGs with UVX. The two objectives in our study are to: 1) use photometry between the UV and mid-IR to constrain the stellar populations contributing to the UV emission, and 2) use radial information to interpret how these galaxies may have assembled their stellar mass.

ETG Sample and Data Analysis. From the *GALEX*-Ultraviolet Atlas of Nearby Galaxies (Gil de Paz et al. 2007), we selected by morphological type E or S0, resulting in a sample of 125 galaxies all at $z < 0.06$. Our final sample resulted in 49 reliable objects, at a mean redshift of 0.02. We present here photometry measured in the *GALEX* FUV/NUV, SDSS r , and *WISE* 3.4 μm bands.

We consider three possible sources for the observed UV excess in ETGs: 1) a significant population of BHB/EHB stars ($t_{\text{age}} > 2$ Gyr and $T_{\text{eff}} > 14000$ K), where EHBs are the combined BHB phase and higher T_{eff} ; 2) a substantial population of hot young stars from a recent starburst ($t_{\text{age}} \lesssim 500$ Myr and $1 < Z < 1.5 Z_{\odot}$, $T_{\text{eff}} > 10000$ K); 3) a significant population of very hot, post main-sequence metal-poor stars ($t_{\text{age}} \gtrsim 9$ Gyr and $Z < 0.5 Z_{\odot}$). We seek to distinguish between these possibilities by comparing their predicted UV/optical/mid-IR colors. To do so, we use the Flexible Stellar Population Synthesis models (FSPS; Conroy et al. 2009; Conroy & Gunn 2010) to create composite stellar population (CSP) models. For a full explanation of sample selection and data analysis see Petty et al. (2013).

2. ETG RADIAL COLOR DISTRIBUTION AND MULTI-STAGE FORMATION

We find strong color gradients for NUV- r , and NUV-[3.4]. By dividing the flux for each galaxy into inner and outer regions (inner half-light, and outer 50–90% of the total flux), we plot in Figure 1-(a) the histograms of NUV- r and

PETTY ET AL.

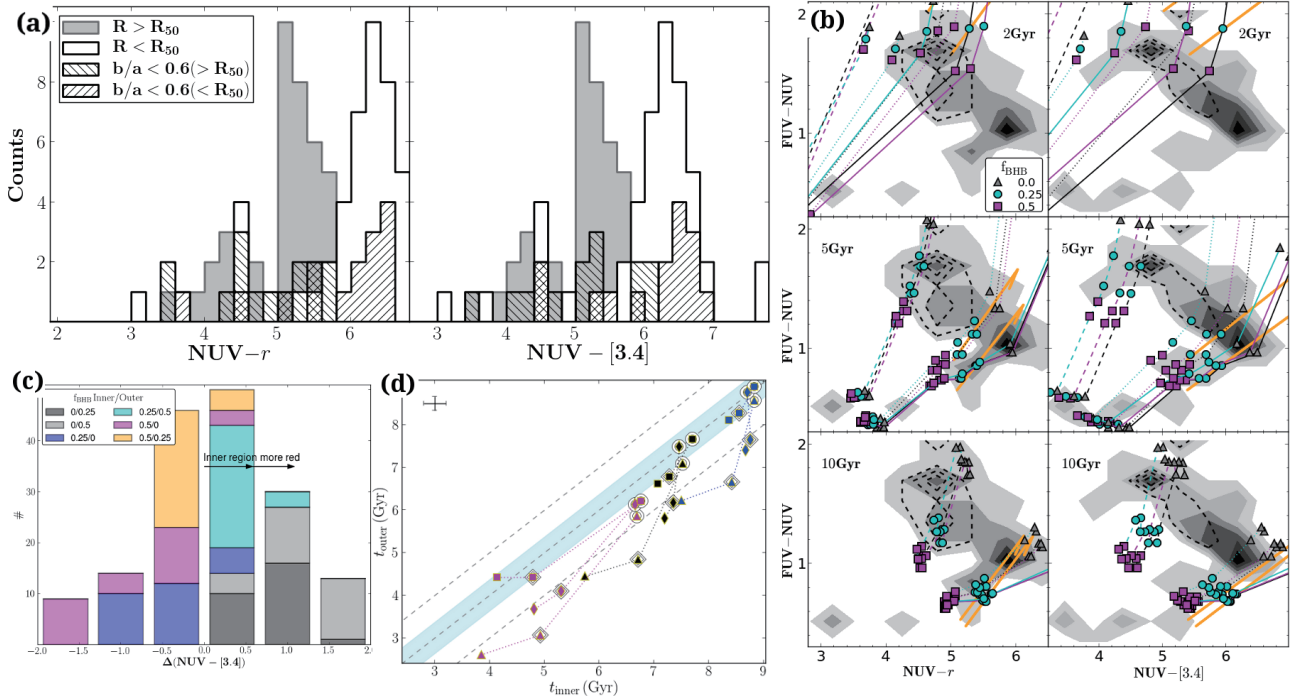


Figure 1. (a) Distributions of $NUV-r$ and $NUV-[3.4]$ colors at the inner half-light (R_{in} , white) and outer radii (R_{out} , grey). The hatches denote a subpopulation of highly elliptical galaxies ($b/a < 0.6$). (b) Color plots with the distribution of inner/outer colors (dashed contour is the outer color distribution). Different parameter combinations of FSPS templates overlay the contours at ages 2 (top), 5 (middle) and 10 (bottom) Gyr. (c) The stacked distributions of $\Delta(NUV-[3.4])$ with different BHB fractions at the inner and outer radii as labeled. For example, the dark grey labeled 0/0.25 refers to the color at $f_{BHB} = 0$ and 0.25 for R_{in} and R_{out} , respectively. (d) Estimated ages for R_{in}/R_{out} considering the different CSP parameter combinations. Symbols are: $\tau = 0.2$ Gyr (black), 0.6 Gyr (blue), and 1 Gyr (magenta); $0.25 Z_{\odot}$ (double circles), $1 Z_{\odot}$ (double diamonds), other $1.5 Z_{\odot}$. The dotted lines trace metallicities along a fixed f_{BHB} and τ with Z .

$NUV-[3.4]$ colors at the inner (R_{in}) and outer (R_{out}) radii, and these show a statistically significant color separation of approximately 1 mag. The averages are: $NUV-r = 5.7 \pm 0.2$ and 4.9 ± 0.1 for R_{in} and R_{out} , respectively; and $NUV-[3.4] = 6.1 \pm 0.2$ and 5.1 ± 0.2 for R_{in} and R_{out} , respectively.

In Figure 1-(b) we take isochrones of the FSPS synthetic photometry at $t_{age} = 2$ (top), 5 (middle), and 10 Gyr (bottom), and plot them in $FUV-NUV$, $NUV-r$, $NUV-[3.4]$ color-space. The FSPS lines overlay the grey-scale contours that include both the R_{in} and R_{out} colors of the ETG sample, and outline the distribution of colors for R_{out} with the dashed contour lines. The density peaks are clearly separated. Dust may be ruled out as the origin of this separation from the direction of the orange vectors. The 2 Gyr plots indicate that the colors for the inner regions could only be explained by super-solar metallicities $> 1.5 Z_{\odot}$. Enforcing the same age across the whole galaxy, then the outer regions are more likely to host a $1-1.5 Z_{\odot}$ stellar population with a moderate BHB fraction. At 5 Gyr (middle plots), the R_{in} colors could be caused by higher metallicity/moderate BHB fractions, and the outer regions would have a lower metallicity and higher numbers of BHBs. At 10 Gyr, the isochrones give narrower ranges and the metallicity dependence is stark: R_{in} would be dominated by $1-1.5 Z_{\odot}$ stellar population and an insignificant BHB fraction; R_{out} would be dominated by a $< 1 Z_{\odot}$ stellar population, and may include slightly more BHBs. We also note that for 2–5 Gyr the dominating SFH is $\tau = 0.2-0.6$; at 10 Gyr the range is widened to all τ .

In Figure 1-(c) we test if BHB fraction can solely cause the 1-mag color difference observed in $NUV-[3.4]$, using estimated ages from fitting the FSPS templates to the ETG colors. The models with BHB fractions $\gtrsim 0.25$ in the **outer radii** are more likely to have a 1-mag color difference (these are shown in light-blue, dark and light grey).

In Figure 1-(d) we show the effects that BHB fraction, metallicity and star formation history have on the estimated ages ($t_{age(in)}$ and $t_{age(out)}$). Each data point is a weighted average of the entire ETG sample, testing different parameter configurations (e.g., one point for $f_{BHB} = 0$, $\tau = 0.2$, and $Z = 1 Z_{\odot}$). We do not separate the temperature boosts here, since Figure 1-(d) indicates that the effects on color are negligible for this analysis.

The points reflect the assumption that both the inner and outer regions are evolving with the same set of parameters. For example, the magenta square ($Z = 1.5 Z_{\odot}$, $f_{BHB} = 0.5$, and $\tau = 1$), easily identified as the outlier, is fixing the prior that the parameter combinations are the same for the inner and outer regions. In other words, each point is the t_{age} coordinate for the inner and outer regions having the same metallicity, BHB fraction, and τ . With this assumption, we find that nearly all points are below the equality line, and many (12 points) with $\Delta t_{age} > 1$ Gyr.

In order for the inner and outer regions to have equal ages, then the inner and outer regions must have a certain set of properties. Over half of the points within errors of the equal age line, have low metallicity (double circles for $Z = 0.25 Z_{\odot}$)

UV-BRIGHT ETGs OBSERVED IN THE MID-IR

and some fraction of BHBs (diamonds and squares). This constrains the possible scenarios that could lead to the observed color difference.

Conclusions. In Petty et al. (2013), the analysis, results and conclusions are discussed in depth. Here we highlight the key results: **I.** *WISE* and *GALEX* colors FUV-NUV and NUV-[3.4] are highly effective in separating the parameters which drive the observed colors. The 49 ETGs in this sample exhibit a strong color difference with bluer colors on the outside of the galaxies in both UV-opt and UV-mid-IR. We extract the photometry for the inner half-light and outer 50–90 % and find a clear color difference: $R_{\text{in}}/R_{\text{out}}$ NUV- $r = 5.7/4.9$, and NUV-[3.4] = 6.1/5.1. **II.** We find that the different regions are significantly different in age, metallicity, and/or the existence of BHBs. We discussed two formation scenarios based on our results: 1) if the bulge and disk coevolved, the metallicities must be significantly different ($0.25 Z_{\odot}$ in the outer regions, $> 1 Z_{\odot}$ in the centers); 2) the ETGs formed in an inside-out process with at least 2 major stages of growth $\gtrsim 1$ Gyr apart. **III.** Our age estimates indicate that the second scenario is most likely. The average ages are estimated to be 7.0 ± 0.3 Gyr (inner) and 6.2 ± 0.2 Gyr (outer), with a minimum of 2.6 Gyr. *Even when we assume homogeneity of parameters over radius, there is evidence of multi-stage evolution where the outer regions are likely to have formed at least ~ 0.8 Gyr after the inner regions ($-0.3 < \Delta t_{\text{age}} < 1.9$ Gyr).* **IV.** Since the estimated ages are beyond the lifetimes of star forming regions to contribute significantly to the UV emission, we assume that BHBs or EHBs are the primary source of the UVX. The average colors fall within the ranges predicted for BHB fractions greater than 0.25 in NUV-[3.4] in the outer regions.

3. SPICA OBSERVATIONS OF ETGS

With the proposed specifications of the Focal Plane Camera, we could achieve much higher resolution and depth than is currently available with *WISE* data. The current sample here could be used as a template for looking at moderate to higher redshift quiescent galaxies. The outer diffuse IR emission of these galaxies is extremely difficult to detect for more distant galaxies, because of significant surface brightness dimming. We could use the FPC for resolved radial profile photometry to try to distinguish at what point these galaxies present a strong color difference between the nucleus and outer regions. Multiple mid-IR filters would more finely disentangle BHB/metallicity degeneracies. Depending on the choice of filters one could, within 0.2 Gyr, create age radial profiles, even with just *GALEX* and *SPICA*.

This publication makes use of data products from the Wide-field Infrared Survey Explorer. The publication is based on observations made with the NASA Galaxy Evolution Explorer.

REFERENCES

- Conroy, C., & Gunn, J. E. 2010, ApJ, 712, 833
 Conroy, C., et al. 2009, ApJ, 699, 486
 Daddi, E., et al. 2005, ApJ, 626, 680
 Gil de Paz, A., et al. 2007, ApJS, 173, 185
 Nelson, E. J., et al. 2012, ApJL, 747, L28
 O'Connell, R. W. 1999, ARA&A, 37, 603
 Petty, S., et al. 2013, AJ, 146, 77